Vibration-Based Propeller Fault Diagnosis for Multicopters

Behnam Ghalamchi[1,2], Mark Mueller[1]

***Abstract*— We present a method for detecting faults in a multicopter's motor/propeller by analysis of the vibration spectrum as measured by an onboard accelerometer. Physical damage to a propeller causes additional vibration in the system during operation, and early detection of such faults may prevent further damage and potentially later catastrophic failure. In the proposed method, only a built-in accelerometer (as typically used by a multicopters flight computer) is used to provide vibration data of the vehicle, and no additional sensors are required. We exploit the fact that the motors rotate at different speeds during different phases of maneuvers, allowing a spectral analysis of measured vibrations to isolate a damaged motor. This method is shown to be effective at identifying multiple damaged propellers as well, and experimental results are presented to validate the concept.**

I. Introduction

Unmanned aerial vehicles are popular with a wide range of applications, and the reliability of these devices is increasingly important as they become more ubiquitous. Because of cost reduction and structural limitations (such as weight or size to attach additional sensors) in many of the commercial products, there is often a lack of structural health monitoring and collision sensing systems. In such a case, using the built-in inertial measurement unit (IMU) which is available in most of the aerial vehicles to provide acceleration information of the vehicle can be a solution to detect some types of structural damage such as propeller issues.

There are many studies available on reliability analysis of UAVs. In simple cases, if there are any fundamental issues as battery low voltage, losing GPS or radio connection from the ground station, a UAV can go to the predefined original point a safe landing mode [1]. A fault detection and diagnosis in electric componenets such as actuators and sensors for unmanned rotary wing vehicles is presented by Zhang et al. [2]. Further studies on actuator failure in quadcopters were investigated in [3] and [4]. They proposed model predictive control which can thus serve as a suitable fault tolerant control approach for a quadcopter. Complete propeller failure of a single propeller of a quadcopter is investigated in [5], [6], and [7], where the strategy is to give up controlling the vehicles yaw angle, and use the remaining propellers to achieve a horizontal spin. Controlling the multicopter experiencing a failure is presented in [8] and [9]. Proposed solutions can be applied as an algorithmic failsafe, allowing, for example, a quadrocopter to fly despite the complete loss of one, two, or three of its propellers.

[1]Mechanical Engineering Department, University of California Berkeley, USA.

[2]Mechanical Engineering Department, Lappeenranta University of Technology, Finland.

{behnam.ghalamchi, mwm}@berkeley.edu

In rotating machinery, structural failures mostly happen on the bearings and rotating wheels such as propellers or impellers. Any defect on rotor bearing system can cause extra vibration during the operations [10], [11]. Another option in structural fault detection is measuring the motors electric current flow. Schoen et. al. [12] and Reily et. al. [13] introduced some application of current spectral analysis to detect the mechanical defect in electric motors. They explained that electric current monitoring can provide the same information as mechanical spectrum analysis without any needs to access to the motor itself. They found the linear relationship between the vibration and current readings. As a result, faulty bearing characteristic frequency was successfully detected by the introduced method.

In case of multicopters, we are dealing with multiple small-scale motors which makes it difficult to investigate the vibration of motors individually. On the other hand, due to the nature of flight, there is always a high level of noise and vibration, that originates from aerodynamic properties and flight stabilization control loop of the UAVs, rather than the motor. Yap [14] presented the structural health monitoring for UAVs, by considering the effects of three possible physical damages such as a broken propeller, loose pylon, and damaged motor mount. micro-electromechanical (MEMS) accelerometers were installed close to the motors in a way to measure vibrations signals more accurately, and a Discrete Fourier Transform (DFT) was used to analyze the data. Out of this work, it can be understood that vibration analysis to detect any defect in UAVs is difficult during the actual flight because of the high level of noise and also vibration transmission between the motors along the structure. Anaya et. al. [15] implemented machine learning into damage classification of fixed-wing UAVs. They used data from piezoelectric transducers attached to the structure to

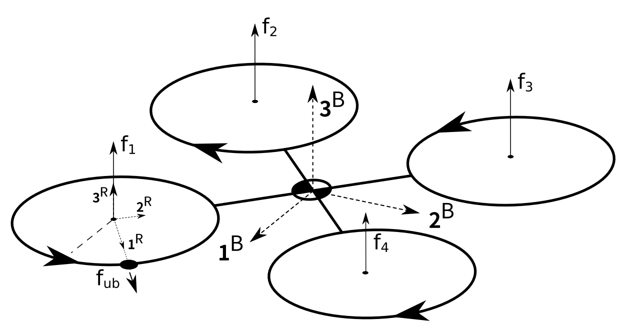

Fig. 1. Diagram of the quadcopter. An unbalance mass located on propeller number 1, thus producing a centrifugal force.

implement the damage classification methodology. Another study on failure detection of small UAVs has been done by Kandaswamy and Balamuralidhar [16]. They used information out of sensors, navigation algorithms, control inputs, and outputs, then post-processing data and compare with available statistical data to detect mechanical or electrical failure.

Lately, Ronay et. al. [17] introduced model-based sensor fault diagnosis for a quadrotor UAV. In order to perform fault detection and isolation, quadrotor modelled as a Linear Parameter Varying (LPV) system. A fault detection and isolation scheme is considered by mean of an observer bank in order to detect and isolate sensor faults. Fault free results is recorded and used to detect and isolate sensor faults in comparison with the predefined threshold.

In this paper, a simple and versatile algorithm is proposed to detect the defective propeller in a quadrotor. Unlike the introduced literature, our method is using a built-in accelerometer which is available in most of the quadrotors, to identifying the damaged propeller. as a consequence, newly developed fault detection algorithm can be implemented to the wide range of quadrotors. Accelerometer data is recorded for several flight trajectories, and by analyzing the vibration spectrum damaged propeller can be identified.

II. Modeling

A simple quadcopter model which we used in this study is shown in Fig. 1. The body-fixed coordinate system defined by the triad $\mathbf{1}^B$, $\mathbf{2}^B$, and $\mathbf{3}^B$. An unbalance mass is located in on one of the propellers which produce a force in a radial direction. The eventual objective is to identify the propeller on which this unbalance is located.

A. Dynamics

Each propeller i produces a thrust force $\boldsymbol{f}_i$ and a torque $\boldsymbol{\tau}_i$ as a function of its rotational speed, Ω_i.

$$\boldsymbol{f}_i = \kappa \Omega_i^2 \boldsymbol{e}_i \tag{1}$$

$$\boldsymbol{\tau}_i = (-1)^i \gamma \boldsymbol{f}_i + \boldsymbol{s}_i \times \boldsymbol{f}_i \tag{2}$$

with κ and γ being aerodynamic constants depending on the propellers. In the body-fixed coordinate system, the unit vector $\boldsymbol{e}_i$ is perpendicular to the propellers planes of rotation as $(0, 0, 1)$. The propeller i is displaced from the vehicles center of mass by $\boldsymbol{s}_i$, and produces a force $\boldsymbol{f}_i$, and a moment about its rotation axis. For instance, the displacements for the propeller with an unbalance mass on it is defined below, introducing a scalar length l,

$$s_1^B = l(+1^B - 2^B) \tag{3}$$

In addition, a radial unbalance force in rotational coordinate ($\boldsymbol{f}_{ub}^R = m\boldsymbol{r} \times \Omega_i^2$) can be reflected to $\mathbf{1}^B$, $\mathbf{2}^B$ vectors as follows:

$$\boldsymbol{f}_{ub,i}^{1B} = \boldsymbol{f}_{ub,i} \sin(\Omega_i t) \tag{4}$$

$$\boldsymbol{f}_{ub,i}^{2B} = -\boldsymbol{f}_{ub,i} \cos(\Omega_i t) \tag{5}$$

where m is the unbalance mass and $\boldsymbol{r}$ is the radial location of the mass. The vehicle's dynamics can be described using the Newton-Euler equations. Translational acceleration $\ddot{\boldsymbol{x}}$, in the earth-fixed coordinate and its angular acceleration $\dot{\boldsymbol{\omega}}$, in the body-fixed frame as below. We introduce the rotation matrix $\boldsymbol{R}$, which relates the body-fixed and world-fixed frames, and introduce the disturbance force $\boldsymbol{f}_d$ and torque $\boldsymbol{\tau}_d$.

$$m\ddot{\boldsymbol{x}} = m\boldsymbol{g} + \kappa \boldsymbol{R} \sum \Omega_i^2 \boldsymbol{e}_i + \boldsymbol{f}_{ub}^B + \boldsymbol{f}_d \tag{6}$$

$$\dot{\boldsymbol{R}} = \boldsymbol{R}[\![\boldsymbol{\omega}]\!] \tag{7}$$

$$\boldsymbol{I}\dot{\boldsymbol{\omega}} = -\boldsymbol{\omega} \times \boldsymbol{I}\boldsymbol{\omega} + \sum \left((-1)^i \gamma \boldsymbol{f}_i + \boldsymbol{r}_i \times \boldsymbol{f}_i\right) + \boldsymbol{\tau}_d \tag{8}$$

III. Fault Diagnosis Method

Mechanical damage in the propellers cause large vibration in the system, due to the unbalanced force from damaged propeller and the high speed with which propellers rotate. In this case, a vibration mode will be excited at each revolution. We propose a technique to identify the fault location in quadrotors at an early stage, allowing the vehicle to take appropriate action (e.g. land) and to prevent further damages to the other components. Furthermore, as the individual motor/propeller that is the source of the vibration is isolated, this may be used for maintenance; in the case of vehicles with actuator redundancy (e.g. octocopters) the damaged propeller may be disabled.

As is proposed in [14], it is relatively straightforward to spot the vibration level of quadrotors in a preflight stage. However, fault diagnosis of multicopters is more complicated in actual flights, due to the external excitation and also the vibration transmission between the motors. In our algorithm, we record accelerometer information, deconstruct signals using the Discrete Fourier transformation (DFT), and compare the vibration spectrum in frequency domain for different flight trajectories to identify the damaged motor.

Fig. 2 shows the quadrotor motor force components that generate desired a motion. At hover, equal forces are produced, meaning that all motors are running almost at similar speeds. To produce the torques required for moving the vehicle to a side requires opposing motors to have a thrust (and thus speed) differential, which may be used to isolate a fault.

We also know that an unbalance mass increases the vibration level of the system. This effect can be seen in a DFT spectrum as a clear peak at rotation frequency of the damaged propeller. This means that, if an unbalance mass is located on a motor which is spinning with the lower speed, the spectrum shows a distinct peak at lower frequency compares with the motor with higher speed. Making several flight trajectory allows motor to spin with different speeds,

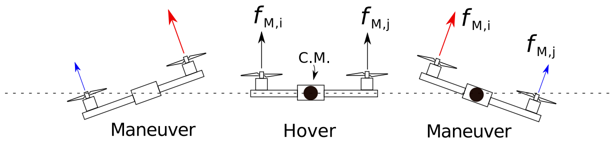

Fig. 2. Motor force components required for different flight motions, showing the imbalance in forces (and thus motor/vibration frequency) when the vehicle maneuvers.

and this help us to identify the damaged motor according to the vibration spectrum analysis and spinning frequency.

Fig. 3 shows the needed flight trajectories to find the location of the damaged propeller. In case of flight stage $S1$, motors $M1$ and $M4$ are running with the same speed and in a mean while $M2$ and $M3$ spinning faster than $M1$ and $M4$.

As a simple case for a quadcopter, if there is an unbalance mass on one of the propellers, in two flight paths ($S1$ and $S2$), and comparing the spectrum outputs, it possible to say on which half of the vehicle this unbalance mass is located ($M1-M4$ or $M2-M3$). Next, this is repeated for two new flight trajectories which are perpendicular to previous ones $S3$ and $S4$. In this section we will learn if the damaged propeller is on $M1-M2$ or $M3-M4$. Unbalance mass should be located at the intersection of these spots.

As is explained earlier, finding a single defected propeller needs four flight stages ($S1$ - $S4$). However, in more complicated cases with more that one damaged actuators, it is needed to have further analysis with having more flight stages ($S5$ - $S8$). Further case studies will be introduced with experimental examples.

IV. Experimental Verification

Fig. 4 shows the quadcopter that was used for experiments. The main reason to use this platform is that it is small (106 mm from the motor to motor) and light (total weight is 44.5 grams include the battery), which makes it easy and safe for indoor experiments.

The control system architecture and test setup facilities are presented in Fig. 5. A motion capture system is used to track the vehicle. The Robot Operating System (ROS) was used for communication and data logging. In this study, a built-in accelerometer is located at the center of the quadcopter body.

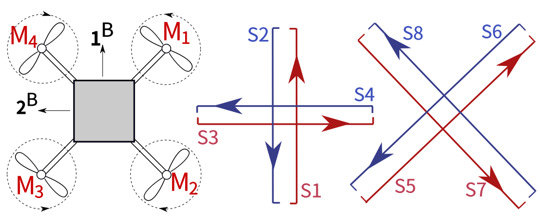

Fig. 3. Identification of motors and flight trajectory components. Identification of single defected propeller needs four flight side flight stages ($S1$ - $S4$), and the identification of multiple damaged propellers additionally requires diagonal trajectories ($S5$ - $S8$)

Fig. 4. The quadcopter used in experiment.

Three case studies will be considered in this paper (see Fig. 6). In Case A, Only one propeller is damaged. In Case B, it is assumed that two propellers are damaged and they are located on the same side of the quadcopter. Finally, in Case C we will consider two faulty propellers located diagonally. To identify the location of a damaged propeller, in each case study we need to have several flights.

In the experiments, a propeller is intentionally unbalanced by removing mass from the propeller's edge (see Figure 7). The unbalance mass applied to the system is equal to 0.005g and is located at 32.5mm from the motor center. Table I shows physical parameters of the quadcopter which have been used in the experiments. For all case studies, accelerometer data in $\mathbf{1}^B$ direction is recorded and vibration spectrum is illustrated for each individual case. A Hanning window is used to reduce spectral leakage and make smoother outputs.

A. Single Damaged Propeller

As a case study, it is assumed one of the propellers has a small cut off at one end. Fig. 6 shows the unbalance mass which is located on motor number 1 ($M1$). According to motor force distributions in Fig. 2, during the motion stage from negative 2^B to positive 2^B, motors are rotating faster in the right-hand side of the quad which means that in FFT

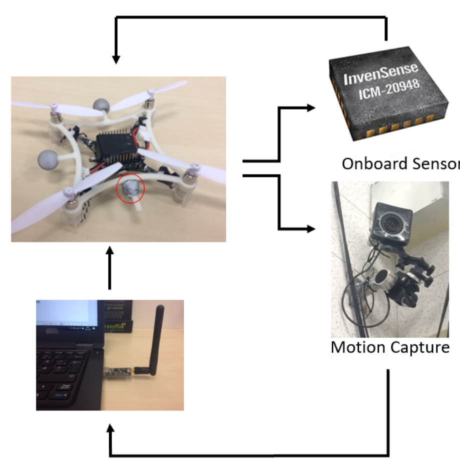

Fig. 5. Experimental Layout: a built-in accelerometer is used to provide vibration data of the vehicle. A motion capture system tracks the vehicle for position control, and telemetry data is transmitted to a laptop computer.

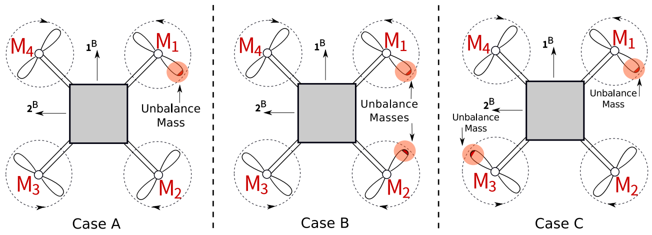

Fig. 6. Three case studies; Case A, single damaged propeller; Case B, two damaged propellers located on the same side; Case C, two damaged propellers located on opposing sides. The unbalance mass is similar in all cases.

TABLE I
PHYSICAL PARAMETERS OF QUADCOPTER

Mass (g)	39
arm length (m)	0.053
angular speed squard to thrust $\frac{Ns^2}{rad^2}$	4.14e-8
aerodynmaic constant for thrust to torque (m)	0.0164
mass moment of inertia around 1^B axis($kg.m^2$)	$30.0e^-6$
mass moment of inertia around 2^B axis($kg.m^2$)	$30.0e^-6$
mass moment of inertia around 3^B axis($kg.m^2$)	$60.0e^-6$

plot clear peaks should be seen in higher frequencies than when we are flying in the opposite direction. The same fact should be seen in the flying in 1^B direction.

Measurement results for 4 flight stages are presented in Fig. 8. Acceleration parameters are recorded for all stages with a sample rate of 500Hz (on-board loop is running at the same rate). Each flight stage has 2m length which should be passed in 2s. We thus measured 1000 points per stage.

Each peak shows an unbalance response at the frequency which is equal to the rotation speed of the motor with a damaged propeller on it. At flight stage 1, $M1$ and $M4$ is rotating slower than $M2$ and $M3$ (231Hz), and at stage 2, the motors are spinning faster (245Hz), Therefore the spectrum at stage 1 shows a peak at a lower frequency, meaning that the unbalance mass is located on either $M1$ or $M4$. Doing the same observation for the stages 3 and 4 gives the unbalance mass location on $M1$ or $M2$, and it means that the faulty propeller is located on intersection of these stages which is on $M1$, which is the correct for predefined unbalance mass location. Also in the measurement results, we can see some vibration in lower frequencies around 100Hz and this is not related to unbalance mass and at this point, it is an unknown phenomena. Also, there is a difference between frequencies in 1^B and 2^B flight stages. This might comes from asymmetry in the quadcopter structure. Even so, the

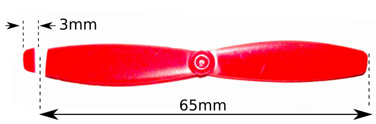

Fig. 7. Damaged Propeller: a small mass is removed from one end of propeller. The propeller's total mass is 0.35g, and the removed mass is approximately 0.005g (that is, less than 2% of the propeller).

motors arm and distribution are perfectly symmetric, but the battery center of mass can be one reason to observe such a difference.

B. Two Broken Propellers - same side

As a second case study, we assumed that two damaged propellers are located on one side of the quadcopter (In this configuration they are on $M1$ and $M2$). According to fig. 9, Flight stages 1 and 2 have similar spectrum. The reason is that the unbalance masses are distributed evenly in both flight stages. Unlike the previous case study, theses stages are not as informative, only telling us that because of the high spectrum amplitude, we have two unbalance masses. Continuing the measurement, flight stage 4 shows a spectrum peak at the higher frequency, which means that two damaged propellers are located at $M1$ and $M2$.

C. Two Broken Propellers - Diagonal

The last case is if there are two damaged propellers are distributed diagonally (In this configuration they are on $M1$ and $M3$). In this particular case, the FFT spectrums for the first four stages are not informative. The reason is at any of these flight stages ($S1$ - $S4$) it would be two defected propeller in opposite side of the flight trajectory, which are spinning with different speed (one side is higher than the other side) which end with FFT spectrum with multiple peaks. As a result, side flight stages are not useful to identify the damaged propellers. It only declare the fact of possibility of having the two damaged propeller in diagonal to each other. That is why we have to define the new flight trajectories where were defined as it shown in Fig. 10. Analyzing the Flight stage 5 ($S5$) as an example of diagonal flight trajectory, it is expecting that $M2$ and $M4$ rotate with he same speed, and $M3$ rotates faster that $M1$. Keeping this assumption and analyzing $S5$ - $S6$ tells that $S5$ and $S6$ has the similar vibration with a peak at higher frequency compare with $S7$ - $S8$. This means that two diagonal unbalance masses are located on $M1$ and $M3$.

V. CONCLUSION

A simple procedure for fault detection in quadcopters propellers was introduced in this study. The concept uses a built-in accelerometer unit to measure the acceleration of a quadcopter and detect the location of a damaged propeller with spectrum comparison for several flight trajectories. Proposed algorithm only works when quadrotor follows predefined trajectory. In the future work, we will work on a model which can be independent from the flight trajectory. Due to the common dynamic behavior of quadrotors, the proposed method can be implemented it to any other quadrotor varying in size. Results were verified by experimental measurement. Experiments have been done in indoor flight arena. However, this can be implemented in outdoor flights. In future, the proposed procedure can be completely autonomous and we plan to make it independent of flight trajectories. This work can be applicable in fault detection in swarm flight which is difficult to do the manual procedure of health monitoring. In

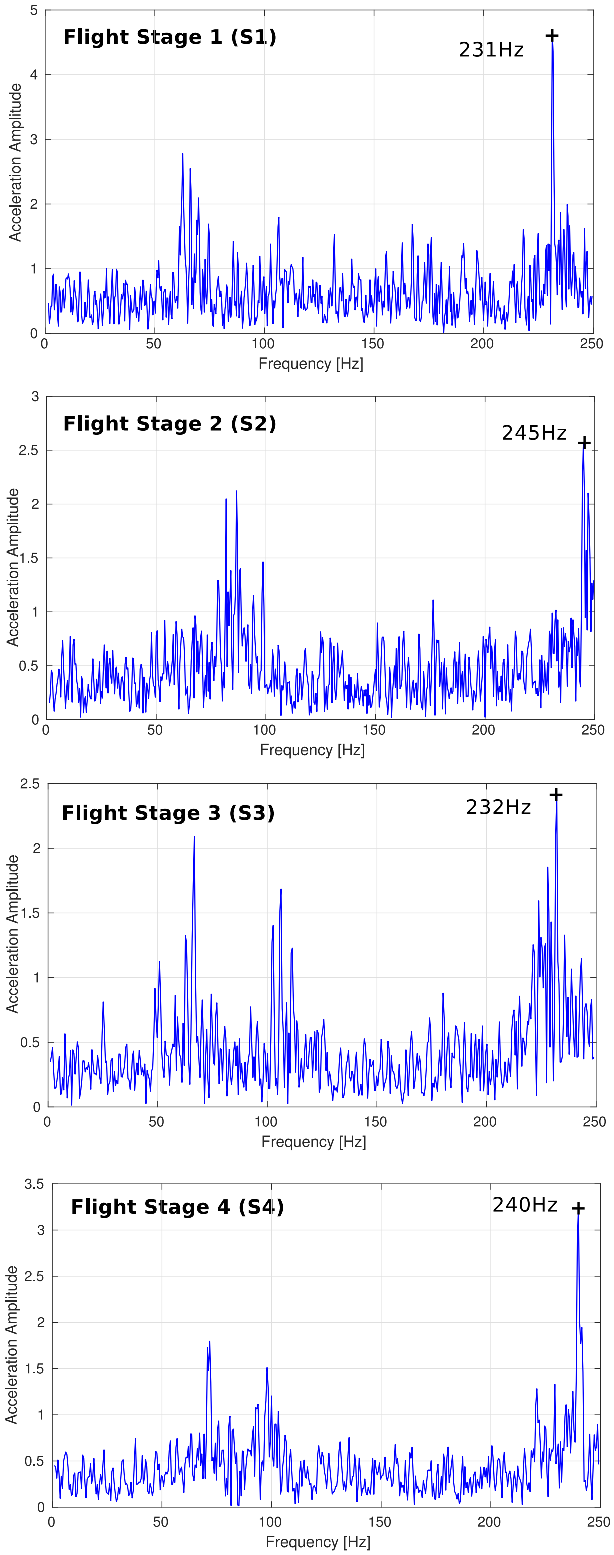

Fig. 8. Four flight stages spectrum for single damaged propeller, Case A, ($S1$ - $S4$). Peak with high amplitude shows the rotation speed of the damaged propeller. At $S1$, $M1$ and $M4$ is spinning slower that $M2$ and $M3$, which is opposite for $S2$. The same for $S2$ and $S3$ where motors in each stage running differently. the faulty propeller is located on intersection of these stages which is on $M1$

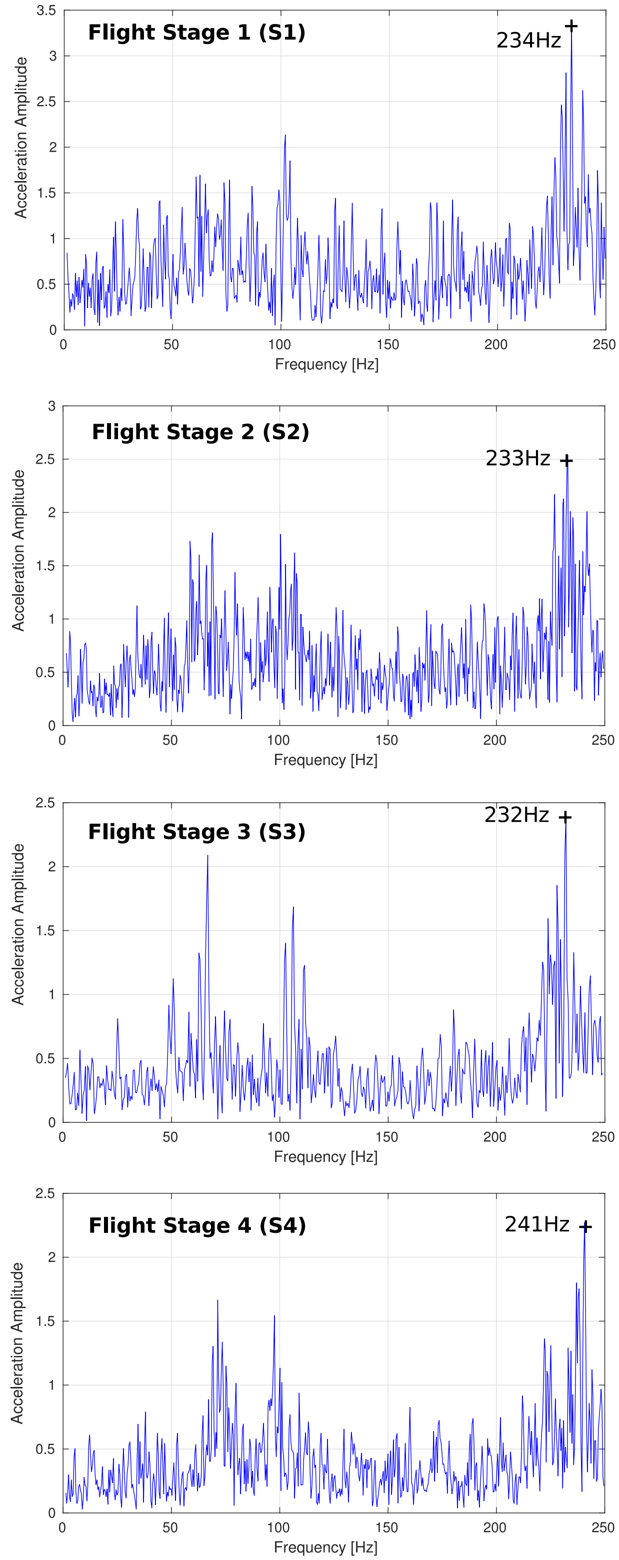

Fig. 9. Four flight stages spectrum for Two Broken Propellers in the same side, Case B. ($S1$ - $S4$). Dynamic of flight stages $S1$ - $S2$ is similar because in both stages there is a similar defected propeller which is spinning similarly. This shows that there are two damaged propeller. $S3$ shows a peak at lower frequency in comparison with $S4$. This means that two damaged propellers are on $M1$ and $M2$

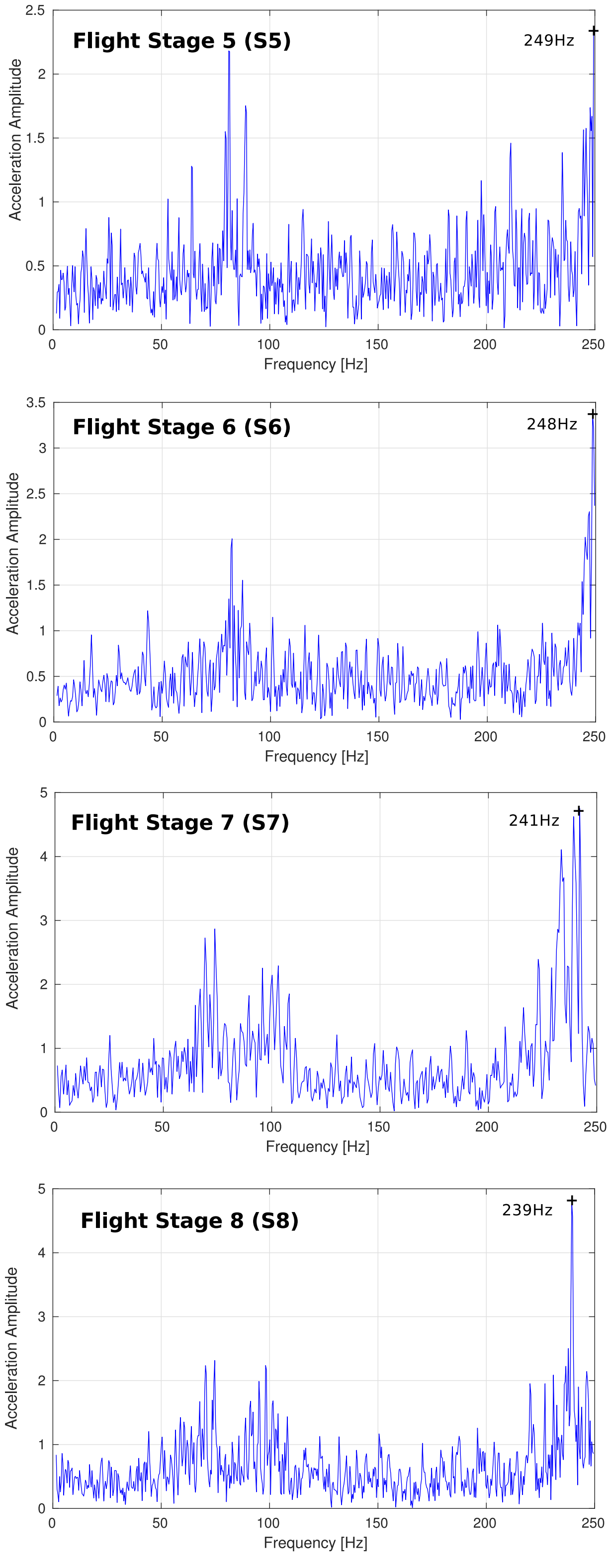

Fig. 10. Four diagonal(cross) flight stages spectrum for Two Broken Propellers in the opposite side, Case C. ($S5$ - $S8$). Analyzing $S5$ - $S6$ tells that $S5$ and $S6$ has the similar vibration with a peak at higher frequency compare with $S7$ - $S8$. This means that two diagonal unbalance masses are located on $M1$ and $M3$.

this paper, we consider the effect of unbalance mass but in future, it can be continued to fault diagnosis of quadrotors from several sources as motor mount damages and motor bearings. There is also a possibility to extend this work on real-time fault detection procedure of quadrotors.

Acknowledgements

This work is partially supported by the Finnish Cultural Foundation - the Foundations Post Doc Pool.

References

[1] G. Parr and P. Morrow, *Sensor Systems and Software: Second International ICST Conference, S-Cube 2010, Miami, FL, December 13-15, 2010, Revised Selected Papers*. Springer, 2011, vol. 57.

[2] Y. Zhang, A. Chamseddine, C. Rabbath, B. Gordon, C.-Y. Su, S. Rakheja, C. Fulford, J. Apkarian, and P. Gosselin, "Development of advanced fdd and ftc techniques with application to an unmanned quadrotor helicopter testbed," *Journal of the Franklin Institute*, vol. 350, no. 9, pp. 2396–2422, 2013.

[3] H. A. Izadi, Y. Zhang, and B. W. Gordon, "Fault tolerant model predictive control of quad-rotor helicopters with actuator fault estimation," *IFAC Proceedings Volumes*, vol. 44, no. 1, pp. 6343–6348, 2011.

[4] M. Ranjbaran and K. Khorasani, "Fault recovery of an under-actuated quadrotor aerial vehicle," in *Decision and Control (CDC), 2010 49th IEEE Conference on*, IEEE, 2010, pp. 4385–4392.

[5] A. Akhtar, S. L. Waslander, and C. Nielsen, "Fault tolerant path following for a quadrotor," in *Decision and Control (CDC), 2013 IEEE 52nd Annual Conference on*, IEEE, 2013, pp. 847–852.

[6] A. Freddi, A. Lanzon, and S. Longhi, "A feedback linearization approach to fault tolerance in quadrotor vehicles," *IFAC Proceedings Volumes*, vol. 44, no. 1, pp. 5413–5418, 2011.

[7] D. Lattanzi and G. R. Miller, "3D scene reconstruction for robotic bridge inspection," *Journal of Infrastructure Systems*, vol. 21, no. 2, p. 04 014 041, 2014.

[8] M. W. Mueller and R. D'Andrea, "Relaxed hover solutions for multicopters: Application to algorithmic redundancy and novel vehicles," *The International Journal of Robotics Research*, vol. 35, no. 8, pp. 873–889, 2016.

[9] M. W. Mueller, S. Lupashin, R. D'Andrea, and M. Waibel, *Controlled flight of a multicopter experiencing a failure affecting an effector*, US Patent 9,856,016, Jan. 2018.

[10] R. Randall, "Detection and diagnosis of incipient bearing failure in helicopter gearboxes," *Engineering Failure Analysis*, vol. 11, no. 2, pp. 177–190, 2004.

[11] B. Ghalamchi, J. Sopanen, and A. Mikkola, "Modeling and dynamic analysis of spherical roller bearing with localized defects: Analytical formulation to calculate defect depth and stiffness," *Shock and Vibration*, vol. 2016, 2016.

[12] R. R. Schoen, T. G. Habetler, F. Kamran, and R. Bartfield, "Motor bearing damage detection using stator current monitoring," *IEEE transactions on industry applications*, vol. 31, no. 6, pp. 1274–1279, 1995.

[13] C. M. Riley, B. K. Lin, T. G. Habetler, and R. R. Schoen, "A method for sensorless on-line vibration monitoring of induction machines," *IEEE transactions on industry applications*, vol. 34, no. 6, pp. 1240–1245, 1998.

[14] Y. K. Yap, "Structural health monitoring for unmanned aerial systems," *EECS., UNC, BerNley, Rep. UCB/EECS-2014-70*, 2014.

[15] M. Anaya, H. Cern, J. Vitola, D. Tibaduiza, and F. Pozo, "Damage classification based on machine learning applications for an un-manned aerial vehicle," *Structural Health Monitoring 2017*, 2017.

[16] G. Kandaswamy and P. Balamuralidhar, "Health monitoring and failure detection of electronic and structural components in small unmanned aerial vehicles,"

[17] F. R. Lpez-Estrada, J.-C. Ponsart, D. Theilliol, Y. Zhang, and C.-M. Astorga-Zaragoza, "Lpv model-based tracking control and robust sensor fault diagnosis for a quadrotor uav," *Journal of Intelligent & Robotic Systems*, vol. 84, no. 1-4, pp. 163–177, 2016.